This article has been accepted for publication in a future issue of this journal, but has not been fully edited. Content may change prior to final publication. Citation information: DOI 10.1109/TII.2017.2787988, IEEE Transactions on Industrial Informatics

Massive MIMO for Industrial Internet of Things in Cyber-Physical Systems

Byung Moo Lee, *Member, IEEE* and Hong Yang, *Senior Member, IEEE*

***Abstract*—To apply Cyber-Physical System (CPS) technique in industrial internet, a wireless technology that is able to robustly maintain hyper connectivity between a data center and distributed UEs (User Entities) and/or IIoT (Industrial Internet of Things) devices is required. We investigate the feasibility of utilizing Massive MIMO (Multi-Input Multi-Output) as such a wireless technology. We analyze the performance of a Massive MIMO base station deployed at a data center to provide massive connectivity to a large number of devices. In addition, we discuss related research challenges for deploying Massive MIMO in industrial internet applications of CPS, such as device scheduling and power control, energy efficient design and RF (Radio Frequency) energy transfer/harvesting, signaling techniques for drones and mobile robots, and applications of underwater industrial internet.**

***Index Terms*—Industrial Internet of Things; Cyber-Physical System; Massive MIMO.**

I. Introduction

Cyber-Physical System (CPS) pursues real-time fusion of the physical world and the cyber world, and it is a core concept of the 4th industrial revolution with the characteristics of hyper-connectivity, hyper-automation and hyper-intelligence [1] [2] [3]. The smart factory is an intelligent and flexible production system that produces customized products in real-time. To increase the competitiveness of the smart factory based manufacturing industry, CPS is to be actively utilized. A CPS for the design and operation of smart factory is called a cyber-physical production system (CPPS). It gathers manufacturing big data, analyzes the data in real time through data analytics, and performs efficient operations of manufacturing systems, thus automatically recognizes changes of orders, processes abnormality, and corrects equipment failures. The application of internet of things (IoT) in industry is called industrial internet of things (IIoT), or industrial internet [4] [5]. For the realization of CPS in manufacturing systems, the industrial internet provides a medium for gathering manufacturing big data.

To apply industrial internet in CPS, various base technologies must be in place. Hyper connectivity precedes others in enhancing both automation and intelligence. To guarantee the hyper-connectivity of CPS, both stationary devices such as sensors used for exchanging and monitoring the status information, and moving devices such as mobile robots and surveillance drones must be connected to the data center using a powerful wireless technology.

Massive multiple-input multiple-output (MIMO) systems have received a great deal of attention in both academia and industry due to its characteristics of huge spectral efficiency (SE) and energy efficiency (EE) [6] [7] [8]. The basic concept of Massive MIMO is generating an excessive amount of channel gain by increasing the number of base station (BS) service antennas as many as we can, to increase both SE and EE with high reliability. With the excessive amount of channel gain, it is possible to use low complexity precoding, scheduling and power allocation due to its distinct channel hardening effect. The 3rd generation partnership project (3GPP) standards body has been actively discussing the inclusion of Massive MIMO in 3GPP specifications from release 13 onward [9].

The concept of Massive MIMO is different from that of traditional MIMO. A traditional MIMO system generally uses almost the same number of transmitter (TX) and receiver (RX) antennas to achieve high channel capacity because the channel capacity can be maximized with the same number of TX/RX antennas from a system configuration perspective. Increasing one side of TX/RX antennas increases power gain, but is of little help in increasing channel capacity. In the internet of things (IoT) era, however, it is impossible to configure the same number of TX antennas at the TX, and RX antennas at the RX because data center and/or base station (BS) can increases the number of TX antennas, while distributed entities and/or IoT devices cannot increase the number of RX antennas due to the space limitation. Multi-user (MU) MIMO systems, which transmit the signal from data center to multiple single-antenna IoT devices, have also been introduced. In this case, precoding and decoding, scheduling and power allocation techniques can be very important, and it is not so easy to efficiently use in real situation due to the complexity of the related optimization schemes. Massive MIMO also transmits signals from one data center to the multiple single-antenna IoT devices. Thus it is also a kind of MU-MIMO system. Unlike the traditional MU-MIMO, Massive MIMO has many more TX antennas at the TX than RX antennas at the RXs, typically it has several times more service antennas than the number of active UE devices that have only one antenna each. Based on the channel gain and the asymptotic orthogonality of channel vectors using many TX antennas, precoding, decoding, scheduling and power allocation schemes become significantly simpler to apply. Based on the characteristics we mentioned above, for the hyper-connectivity of CPS, Massive MIMO can play a key role as a core technology.

Manuscript received August 30, 2017; revised November 26, 2017; accepted December 13, 2017. This research was supported by Basic Science Research Program through the National Research Foundation of Korea (NRF) funded by the Ministry of Education (NRF-2017R1D1A1B03028350).

B. M. Lee is with the School of Intelligent Mechatronics Engineering, Sejong University, Seoul, 05006, South Korea, e-mail:blee@sejong.ac.kr.

H. Yang is with the Mathematics of Networks and Communications Research Department, Nokia Bell Labs, Murray Hill, NJ 07974 USA, e-mail:h.yang@nokia-bell-labs.com.

This article has been accepted for publication in a future issue of this journal, but has not been fully edited. Content may change prior to final publication. Citation information: DOI 10.1109/TII.2017.2787988, IEEE Transactions on Industrial Informatics

In this paper, we introduce the industrial internet application of CPS using Massive MIMO. Even though Massive MIMO has received a great deal of attention due to its distinct characteristics, there are few studies applying its concept to CPS. Fundamentally, Massive MIMO is well-suited to support distributed IoT devices because it has a large number of service antennas, can easily support distributed UEs, and thus it can realize the hyper-connectivity for CPS. There are two main objectives for this paper. First, we show the feasibility of using Massive MIMO for the massive IIoT device connectivity. Moving one step further from traditional Massive MIMO we mentioned, we consider a Massive MIMO system that serves a much larger number of distributed IIoT devices than its number of service antennas in a single cell scenario. In the case of supporting excessive amount of IIoT devices, due to limited resources, reference signal (RS) reuse in a single cell may be applied depending on situations. This is a new operating paradigm for Massive MIMO. We present several numerical results for a Massive MIMO system with massive connectivity. Our results show that for both uplink and downlink, the total spectral efficiency (SE) can continue to increase as the number of IIoT devices K increases beyond the number of service antennas M. This means Massive MIMO can provide great benefits for the system requiring low power and moderate data rate, even in the situation of supporting very large number of IIoT devices. Next, we discuss possible research topics for CPS using Massive MIMO, such as scheduling, high energy efficiency design, radio frequency (RF) based energy harvesting, support of signaling and auto-landing for surveillance drone, etc. The underwater industrial internet is also a growing field due to the increase of various underwater works, for example underwater farm management, offshore oil/gas development, and underwater robot work. Various applications introduced in this paper can be of great help for further investigations.

Overall, this paper aims to provide a comprehensive introduction on the industrial internet applications of CPS using Massive MIMO. This is a timely and essential topic to deal with, because the true IoT era is about to begin, so it is necessary to design a highly reliable communication system that can support massive connectivity.

In what follows, the Massive MIMO system model is described in Section II. The basic concept of Massive MIMO to support many IIoT devices, and RS reuse based system performance are shown in Section III. Possible research topics and challenges are discussed in Section IV, and conclusions are given in Section V.

II. Massive MIMO System

Let $\mathbb{R}_+$ denote the set of all positive real numbers, and let $\mathbb{R}_{0+} = \{0\} \cup \mathbb{R}_+$. Let $\mathbb{R}_+^n$, $\mathbb{R}_{0+}^n$, $\mathbb{R}_+^{m\times n}$ and $\mathbb{R}_{0+}^{m\times n}$ denote the corresponding n-dimensional and $(m\times n)$-dimensional product spaces. Replacing $\mathbb{R}$ with $\mathbb{C}$ denotes the corresponding complex spaces.

Superscripts: T, *, and † denote matrix transpose, matrix (un-transposed) conjugate, and matrix conjugate transpose respectively.

$\mathbb{E}[\cdot]$ denotes mathematical expectation.

Let

$$G \triangleq [\mathbf{g}_1 \quad \cdots \quad \mathbf{g}_K] \in \mathbb{C}^{M\times K},$$

be the $M \times K$ channel matrix between the M-antenna array at the base station (BS) in a data center and the K active IIoT devices or user entities (UEs). The downlink data channel is modeled as

$$\mathbf{y} = \sqrt{\rho_\mathrm{d}} G^\mathrm{T}\mathbf{x} + \mathbf{w}, \tag{1}$$

where $\mathbf{y} \in \mathbb{C}^K$ is the received signal vector at the K UE receivers, ρ_d is the downlink signal power, $\mathbf{x} \in \mathbb{C}^M$ is the power controlled precoded input vector to the M-antenna ports in the BS, and $\mathbf{w}$ is the noise vector. The downlink power constraint is specified as

$$\mathbb{E}[\mathbf{x}^\dagger\mathbf{x}] \le 1. \tag{2}$$

Similarly, denoting the corresponding variables with a superscript $'$, the uplink data channel is modeled as

$$\mathbf{y}' = \sqrt{\rho_\mathrm{u}} G\mathbf{x}' + \mathbf{w}', \tag{3}$$

where $\mathbf{y}' \in \mathbb{C}^M$ is the received signal vector at the M-antenna ports in the BS, ρ_u is the uplink signal power, $\mathbf{x}' \in \mathbb{C}^K$ is the power controlled message-bearing signal from the K UEs, and $\mathbf{w}'$ is the noise vector. Uplink power constraint is specified as

$$\|\mathbb{E}[\mathbf{x}'^* \odot \mathbf{x}']\|_\infty \le 1,$$

where $\odot$ denotes the element-wise multiplication.

The channel vector between the kth UE and the M-antenna array is modeled as

$$\mathbf{g}_k \triangleq \sqrt{\beta_k}\mathbf{h}_k, \quad k = 1, \cdots, K \tag{4}$$

where β_k is the large-scale fading, and $\mathbf{h}_k$ constitutes the small-scale fading. Let

$$H \triangleq [\mathbf{h}_1 \quad \cdots \quad \mathbf{h}_K],$$

We assume that the UE data symbols $\mathbf{q} \in \mathbb{C}^K$ have zero mean and unit variance, and are uncorrelated

$$\mathbb{E}[\mathbf{q}\mathbf{q}^\dagger] = I_K, \tag{5}$$

and Gaussian noise with

$$\mathbb{E}[\mathbf{w}\mathbf{w}^\dagger] = \sigma_d I_K, \quad \mathbb{E}[\mathbf{w}'\mathbf{w}'^\dagger] = \sigma_u I_M, \tag{6}$$

where I_K and I_M are K-dimensional and M-dimensional identity matrices.

We have

$$G = H \cdot \mathrm{diag}\left[\beta_1^{1/2}, \cdots, \beta_K^{1/2}\right]. \tag{7}$$

For rich scattering, the small-scale fading channel matrix H is modeled by iid (independent and identically distributed) Rayleigh fading.

The well-known linear precoder/decoder for maximum-ratio (MR) processing, zero-forcing (ZF), and minimum mean square error (MMSE) processing, and the associated power control coefficients can be readily formulated as follows.

This article has been accepted for publication in a future issue of this journal, but has not been fully edited. Content may change prior to final publication. Citation information: DOI 10.1109/TII.2017.2787988, IEEE Transactions on Industrial Informatics

A. MR Processing

1) MR Downlink: For MR precoding, we have

$$\mathbf{x} = H^* D_{H^\dagger H}^{-1/2} D_\eta^{1/2} \mathbf{q}, \tag{8}$$

where the diagonal matrices

$$\begin{aligned} D_{H^\dagger H}^{-1/2} &\triangleq \mathrm{diag}\left[\|\mathbf{h}_1\|_2^{-1}, \cdots, \|\mathbf{h}_K\|_2^{-1}\right] \\ D_\eta^{1/2} &\triangleq \mathrm{diag}\left[\eta_1^{1/2}, \cdots, \eta_K^{1/2}\right]. \end{aligned} \tag{9}$$

Here $\boldsymbol{\eta} = [\eta_1 \quad \cdots \quad \eta_K]^{\mathrm{T}}$ is the downlink power control. $\boldsymbol{\eta}$ must satisfy the total power constraint,

$$\boldsymbol{\eta} \in \mathbb{R}_{0+}^K \text{ and } \|\boldsymbol{\eta}\|_1 \leq 1, \tag{10}$$

Then, from (1), we have

$$\mathbf{y} = \sqrt{\rho_{\mathrm{d}}} G^T H^* D_{H^\dagger H}^{-1/2} D_\eta^{1/2} \mathbf{q} + \mathbf{w}, \tag{11}$$

Assuming the MR precoding matrix as $F_d^{\mathrm{mr}} = H^* D_{H^\dagger H}^{-1/2} D_\eta^{1/2}$, (11) is simplified as:

$$\mathbf{y} = \sqrt{\rho_{\mathrm{d}}} \cdot G^T \cdot F_d^{\mathrm{mr}} \cdot \mathbf{q} + \mathbf{w}. \tag{12}$$

2) MR Uplink: For MR decoding, the decoding matrix is $H^\dagger$. From (3) we have

$$H^\dagger \mathbf{y}' = \sqrt{\rho_{\mathrm{u}}} H^\dagger G \mathbf{x}' + H^\dagger \mathbf{w}', \tag{13}$$

where $\mathbf{x}' = D_\eta^{1/2} \mathbf{q}'$ is the power controlled message-bearing signal vector from the K UEs. The uplink power control $\boldsymbol{\eta} = [\eta_1 \quad \cdots \quad \eta_K]^{\mathrm{T}}$ must satisfy the individual power constraint

$$\boldsymbol{\eta} \in \mathbb{R}_{0+}^K \text{ and } \|\boldsymbol{\eta}\|_\infty \leq 1. \tag{14}$$

Assuming the MR processing matrix as $F_u^{\mathrm{mr}} = H^\dagger$, (13) is simplified as:

$$F_u^{mr} \cdot \mathbf{y}' = \sqrt{\rho_{\mathrm{u}}} \cdot F_u^{\mathrm{mr}} \cdot G \mathbf{x}' + F_u^{\mathrm{mr}} \cdot \mathbf{w}' \tag{15}$$

Unlike the downlink case, in the uplink case, there is noise enhancement due to the processing matrix.

B. ZF Processing

1) ZF Downlink: For zero-forcing precoding, we have

$$\mathbf{x} = \sqrt{c_1} H^* (H^{\mathrm{T}} H^*)^{-1} D_\eta^{1/2} \mathbf{q}, \tag{16}$$

With the assumption (5) and the power constraint (2), we calculate that

$$c_1 = \frac{1}{\sum_{l=1}^K [(H^\dagger H)^{-1}]_{l,l} \eta_l}, \tag{17}$$

where $[\cdot]_{l,l}$ denotes the lth diagonal element of a matrix, and $\boldsymbol{\eta} = [\eta_1 \quad \cdots \quad \eta_K]^{\mathrm{T}}$ is the downlink power control. $\boldsymbol{\eta}$ must satisfy the total power constraint (10). Then, from (1), we have

$$\mathbf{y} = \sqrt{\rho_{\mathrm{d}}} G^T \sqrt{c_1} H^* (H^{\mathrm{T}} H^*)^{-1} D_\eta^{1/2} \mathbf{q} + \mathbf{w}. \tag{18}$$

Assuming the ZF precoding matrix as $F_d^{\mathrm{zf}} = \sqrt{c_1} H^* (H^{\mathrm{T}} H^*)^{-1} D_\eta^{1/2}$, (18) is simplified as:

$$\mathbf{y} = \sqrt{\rho_{\mathrm{d}}} \cdot G^T \cdot F_d^{\mathrm{zf}} \cdot \mathbf{q} + \mathbf{w}. \tag{19}$$

2) ZF Uplink: For ZF decoding, the decoding matrix is $(H^\dagger H)^{-1} H^\dagger$. From (3) we have

$$(H^\dagger H)^{-1} H^\dagger \mathbf{y}' = \sqrt{\rho_{\mathrm{u}}} (H^\dagger H)^{-1} H^\dagger G \mathbf{x}' + (H^\dagger H)^{-1} H^\dagger \mathbf{w}', \tag{20}$$

where $\mathbf{x}' = D_\eta^{1/2} \mathbf{q}'$ is the power controlled message-bearing signal vector from the K user terminals. The uplink power control $\boldsymbol{\eta} = [\eta_1 \quad \cdots \quad \eta_K]^{\mathrm{T}}$ must satisfy the individual power constraint (14). Assuming the ZF processing matrix as $F_u^{\mathrm{zf}} = (H^\dagger H)^{-1} H^\dagger$, (20) is simplified as:

$$F_u^{\mathrm{zf}} \cdot \mathbf{y}' = \sqrt{\rho_{\mathrm{u}}} \cdot F_u^{\mathrm{zf}} \cdot G \mathbf{x}' + F_u^{\mathrm{zf}} \cdot \mathbf{w}'. \tag{21}$$

C. MMSE Processing

MMSE processing can be considered instead of ZF processing when SNR is low.

1) MMSE Downlink: For MMSE precoding, we have

$$\mathbf{x} = \sqrt{c_2} H^* \left(H^{\mathrm{T}} H^* + \Gamma_d^{-1} I_K\right)^{-1} D_\eta^{1/2} \mathbf{q} \tag{22}$$

where $\Gamma_d^{-1} \triangleq \mathrm{diag}\left[\frac{\sigma_d}{\rho_{\mathrm{d,1}}}, \cdots, \frac{\sigma_d}{\rho_{\mathrm{d,K}}}\right]$ is the downlink inverse signal-to-noise ratio (SNR) matrix, and $\rho_{\mathrm{d,i}}$ is the downlink signal power to ith UE. With the assumption (5) and the power constraint (2), we calculate that

$$c_2 = \frac{1}{\sum_{l=1}^K [\left(H^{\mathrm{T}} H^* + \Gamma_d^{-1} I_K\right)^{-1} H^{\mathrm{T}} H^* \left(H^{\mathrm{T}} H^* + \Gamma_d^{-1} I_K\right)^{-1}]_{l,l} \eta_l} \tag{23}$$

where $[\cdot]_{l,l}$ denotes the lth diagonal element of a matrix, and $\boldsymbol{\eta} = (\eta_1 \quad \cdots \quad \eta_K)^{\mathrm{T}}$ is the downlink power control. $\boldsymbol{\eta}$ must satisfy the total power constraint (10). Then, from (1), we have

$$\mathbf{y} = \sqrt{\rho_{\mathrm{d}}} G^T \sqrt{c_2} H^* \left(H^{\mathrm{T}} H^* + \Gamma_d^{-1} I_K\right)^{-1} D_\eta^{1/2} \mathbf{q} + \mathbf{w}, \tag{24}$$

Assuming the MMSE procoding matrix as $F_d^{mmse} = \sqrt{c_2} H^* \left(H^{\mathrm{T}} H^* + \Gamma_d^{-1} I_K\right)^{-1} D_\eta^{1/2}$, (24) is simplified as:

$$\mathbf{y} = \sqrt{\rho_{\mathrm{d}}} \cdot G^T \cdot F_d^{mmse} \cdot \mathbf{q} + \mathbf{w}, \tag{25}$$

2) MMSE Uplink: For MMSE decoding, the decoding matrix is $\left(H^\dagger H + \Gamma_u^{-1} I_K\right)^{-1} H^\dagger$, where $\Gamma_u^{-1} \triangleq \mathrm{diag}\left[\frac{\sigma_u}{\rho_{\mathrm{u,1}}}, \cdots, \frac{\sigma_u}{\rho_{\mathrm{u,K}}}\right]$ is the uplink SNR matrix, and $\rho_{\mathrm{u,i}}$ is the uplink signal power from ith UE. From (3) we have

$$\begin{aligned} &\left(H^\dagger H + \Gamma_u^{-1} I_K\right)^{-1} H^\dagger \mathbf{y}' = \\ &\sqrt{\rho_{\mathrm{u}}} \left(H^\dagger H + \Gamma_u^{-1} I_K\right)^{-1} H^\dagger G \mathbf{x}' + \left(H^\dagger H + \Gamma_u^{-1} I_K\right)^{-1} H^\dagger \mathbf{w}' \end{aligned} \tag{26}$$

Assuming the MMSE processing matrix as $F_u^{mmse} = \left(H^\dagger H + \Gamma_u^{-1} I_K\right)^{-1} H^\dagger$, (26) is simplified as:

$$F_u^{mmse} \cdot \mathbf{y}' = \sqrt{\rho_{\mathrm{u}}} \cdot F_u^{mmse} \cdot G \mathbf{x}' + F_u^{mmse} \cdot \mathbf{w}' \tag{27}$$

The three representative processing matrices shown in this section will be used for the performance analysis in next section.

All the downlink/uplink precoding/processing matrices are summarized in Table I.

This article has been accepted for publication in a future issue of this journal, but has not been fully edited. Content may change prior to final publication. Citation information: DOI 10.1109/TII.2017.2787988, IEEE Transactions on Industrial Informatics

TABLE I
DOWNLINK/UPLINK PRECODING/PROCESSING MATRICES

Downlink			Uplink		
MR	ZF	MMSE	MR	ZF	MMSE
$H^* D_{H^\dagger H}^{-1/2} D_\eta^{1/2}$	$\sqrt{c_1} H^* (H^{\mathrm{T}} H^*)^{-1} D_\eta^{1/2}$	$\sqrt{c_2} H^* \left(H^{\mathrm{T}} H^* + \Gamma_d^{-1} I_K \right)^{-1} D_\eta^{1/2}$	$H^\dagger$	$(H^\dagger H)^{-1} H^\dagger$	$\left(H^\dagger H + \Gamma_u^{-1} I_K \right)^{-1} H^\dagger$

III. MASSIVE MIMO FOR IIOT

In this section, we use the framework described in Section II to study the performance of Massive MIMO for IIoT. We assume that there is one data center and K active IIoT devices or user entities (UEs). The data center is equipped with a Massive MIMO antenna system to gather the data from the distributed IIoT devices, and to check the status of operation, after that to transmit data to the distributed IIoT devices to generate timely and high precision operations. IIoT devices or UEs include not only sensors that attached to each industrial machine, but also mobile robots and/or surveillance drones that perform necessary mobile works. The data center has M service antennas, and each UE has one antenna.

Let us consider Massive MIMO systems that support massive IIoT devices. Massive MIMO systems generally use the time division duplex (TDD) mode to reduce the reference signal (RS) overhead. TDD mode shares the same frequency band by sending the uplink and downlink signals during different time slots. There is another popular duplex mode which is called frequency division duplex (FDD). FDD mode divides the uplink and downlink channels based on separate frequency bands. With the TDD mode, channel state information at the TX (CSIT) can be obtained from the uplink RSs without any special feedback from the UEs. Thus we take advantage of channel reciprocity which results in the significant reduction in RS overhead. This is due to the fact that electromagnetic waves traveling in both directions with the same frequency band undergo substantially the same physical phenomena such as reflection, diffraction, and blockage, etc.

Massive MIMO systems assume large M to take advantage of the channel hardening effect [10], i.e., when M is large, all the UE channel conditions become almost deterministic, and scheduling and power control become very simple. In addition, a typical Massive MIMO also assumes $M \gg K$ to provide large throughput to each UE. However, this setup could not be valid to support IIoT, because there could be many IIoT devices that need to be supported coincidently with little delay.

We consider a Massive MIMO system with a large M, and a much larger K. This system can be called a Massive MIMO with massive connectivity. Since K is larger than M, resource allocation for the RS can be a problem even though we use the time division dulplex (TDD) mode. RS contamination is a serious problem in multicell Massive MIMO systems [6]. In the IIoT assumption, single cell could be enough to support the IIoT devices depending on applications. From a practical point of view, for a specific application of IIoT, the intended coverage region is most likely limited to specific areas such as a factory, a construction site, or an educational or research campus, etc., where a single cell can provide adequate coverage.

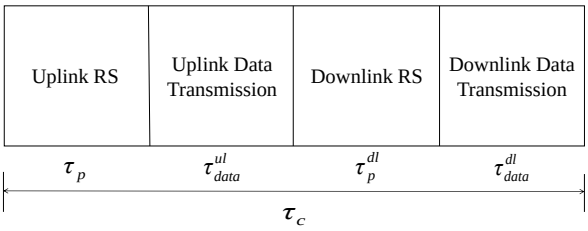

Fig. 1. Resource allocation in TDD mode.

Assuming single cell scenario, due to the large amount of IIoT devices, orthogonal RS resources are reused. In particular, for the system that must maintain the connection continuously for all coherence time and frequency resources, it can be difficult to apply scheduling such as time division multiple access and/or frequency division multiple access, etc. For this reason, we consider the system in which all devices transmit/receive signals in every coherence time/frequency interval. This system setup is applicable to the IIoT where there are many low powered devices to be served simultaneously with little delay.

The simplified uplink/downlink resource allocation in TDD mode is shown in Fig. 1. First, uplink RSs are transmitted from distributed IIoT devices to estimate the uplink channel of each devices. The time duration for the uplink RS is τ_p. Then, the uplink data is transmitted from distributed IIoT devices. Since there are a quite large number of IIoT devices, the uplink data can be a source of big data analysis. The time duration for uplink data transmission is τ_{data}^{ul}. After that, downlink signal transmission from the data center to the distributed IIoT devices should be performed, and the time duration for downlink RS is τ_p^{dl}. The τ_p^{dl} can be minimized using the channel hardening effect. Lastly, the downlink data is transmitted from data center to distributed IIoT devices, and the time duration is τ_{data}^{dl}. All uplink and downlink signal transmissions with RSs should be performed within a coherence time interval, τ_c, within which the communication channel remains substantially constant.

Since we consider the systems which have many IIoT devices, K can be much greater than M and τ_c. Resource scheduling is a possible option, but we consider the system which requires little delay, and thus the signal transmission/reception is performed at least one time within every coherence time and frequency resources. For the systems, we consider the scheme of RS reuse based Massive MIMO with massive connectivity. In this study, we consider J UEs within each group, and UEs use the same uplink RS for channel estimation among different groups, but send and receive individual data. Then, the number

This article has been accepted for publication in a future issue of this journal, but has not been fully edited. Content may change prior to final publication. Citation information: DOI 10.1109/TII.2017.2787988, IEEE Transactions on Industrial Informatics

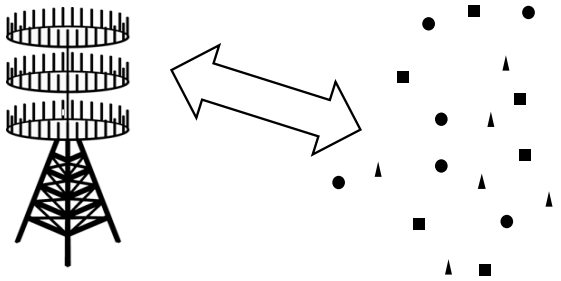

Fig. 2. An example of RS reuse Massive MIMO with massive connectivity, $J=3$, $L=6$, $K=JL=18$ assuming the same shape of IIoT devices use the same RS.

of groups can be $L=\lceil K/J \rceil$. An example of RS reuse Massive MIMO with massive connectivity is shown in Fig. 2. This is the case of $J=3$, $L=6$, $K=JL=18$ assuming the same shape of IIoT devices use the same RS sequences.

From (3), the uplink received RS, $Y_{rs}^{'} \in \mathbb{C}^{M\times\tau_p}$, can be represented as

$$\begin{aligned} Y_{rs}^{'} &= \sum_{i=1}^{L} \sqrt{\rho_{\mathrm{u}}} G_i X_{rs,i}^{'} + W^{'} \\ &= \sum_{i=1}^{L} \sqrt{\tau_p \rho_{\mathrm{u}}} G_i \left(\Phi_{rs,i}^{u}\right)^{\dagger} + W^{'}, \end{aligned} \tag{28}$$

where G_i is the channel matrix for ith group, $\Phi_{rs,i}^{u} \in \mathbb{C}^{\tau_p \times J}$ is the uplink RS matrix for ith group, and if we assume we use orthogonal RS, the uplink RS matrix can be represented as

$$\Phi_{rs,i}^{u} = \left[\boldsymbol{\phi}_{i,1} \ \boldsymbol{\phi}_{i,2} \ \cdots \ \boldsymbol{\phi}_{i,J}\right], \tag{29}$$

where $\boldsymbol{\phi}_{i,k} \in \mathbb{C}^{\tau_p}$ is the RS sequence used by kth UE. Here we assume that $K=JL$ and all groups have the same number of UEs, J. The RS matrix satisfies $\left(\Phi_{rs,i}^{u}\right)^{\dagger} \Phi_{rs,i}^{u} = I_J$, and the RS sequence satisfies $\boldsymbol{\phi}_{i,k}^{\dagger} \boldsymbol{\phi}_{i,l} = 0$, $k \neq l$. Collectively, UEs transmit a $J \times \tau_p$ RS signal, $X_{rs,i} = \sqrt{\tau_p}\left(\Phi_{rs,i}^{u}\right)^{\dagger}$ which is normalized so that each UE extends a total energy that is equal to the duration of RS sequence, $\tau_p \boldsymbol{\phi}_{i,k}^{\dagger} \boldsymbol{\phi}_{i,k} = \tau_p$.

The RS sequences are reused for different groups. For example, the RS sequence of UE k in a group i is the same as the RS sequence of UE l in a group j, i.e., $\Phi_{rs,1}^{u} = \Phi_{rs,2}^{u} =, \cdots = \Phi_{rs,L}^{u}$. Then, from (28), the uplink received RS when the RS sequence is reused for different groups can be represented as

$$\begin{aligned} Y_{rs}^{'} &= \sqrt{\tau_p \rho_{\mathrm{u}}} \left(G_1 (\Phi_{rs,1}^{u})^{\dagger} + G_2 (\Phi_{rs,2}^{u})^{\dagger} + \cdots + G_L (\Phi_{rs,L}^{u})^{\dagger}\right) + W^{'} \\ &= \sqrt{\tau_p \rho_{\mathrm{u}}} \left(G_1 + G_2 + \cdots + G_L\right) (\Phi_{rs,1}^{u})^{\dagger} + W^{'}, \end{aligned} \tag{30}$$

The combined channel information is captured at the RX, and to prevent outage, we should make all the RX SNRs the same using appropriate power control.

As witnessed from previous section, there are three representative detectors for the uplink signal which can be shown as follows.

$$F_{\mathrm{u}} = \begin{cases} \hat{H}^{\dagger} & \text{for MRC} \\ (\hat{H}^{\dagger}\hat{H})^{-1}\hat{H}^{\dagger} & \text{for ZF} \\ \left(\hat{H}^{\dagger}\hat{H} + \Gamma_u^{-1} I_K\right)^{-1} \hat{H}^{\dagger} & \text{for MMSE} \end{cases} \tag{31}$$

where $\hat{H}$ is the estimated channel from uplink RS, and $F_{\mathrm{u}}^{\mathrm{T}} = [\mathbf{f}_{u,1}\mathbf{f}_{u,2}\cdots\mathbf{f}_{u,K}] \in \mathbb{C}^{M\times K}$ is the uplink processing matrix.

Then, the RX signal in the data center for kth UE can be represented as

$$\begin{aligned} \mathbf{f}_{u,k} \cdot \mathbf{y}^{'} &= \sum_{i=1}^{K} \sqrt{\rho_{\mathrm{u,i}}} \mathbf{f}_{u,k} \cdot \mathbf{g}_i x_i^{'} + \mathbf{f}_{u,k} \cdot \mathbf{w}^{'} \\ &= \underbrace{\sqrt{\rho_{\mathrm{u,k}}} \mathbf{f}_{u,k} \cdot \mathbf{g}_k x_k^{'}}_{\text{Desired signal}} + \underbrace{\sum_{\substack{i=1 \\ i\neq k}}^{K} \sqrt{\rho_{\mathrm{u,i}}} \mathbf{f}_{u,k} \cdot \mathbf{g}_i x_i^{'}}_{\text{Inter-User Interference}} + \underbrace{\mathbf{f}_{u,k} \cdot \mathbf{w}^{'}}_{\text{Noise}}, \end{aligned} \tag{32}$$

where $\rho_{\mathrm{u,i}} = \rho_{\mathrm{u}} \eta_i$ is the TX power from ith UE. The SINR is expressed as desired signal power term divided by interference signal power plus noise power.

$$\mathrm{SINR} = \frac{\text{desired signal power}}{\text{interference power} + \text{noise power}}, \tag{33}$$

Based on (32), we can derive the uplink SINR for kth UE [11] [12] [13].

$$\mathrm{SINR}_{\mathrm{k}}^{\mathrm{ul}} = \frac{\rho_{\mathrm{u,k}} \left|\mathbf{f}_{u,k}\mathbf{g}_k\right|^2}{\sum\limits_{\substack{i=1 \\ i\neq k}}^{K} \rho_{\mathrm{u,i}} \left|\mathbf{f}_{u,k}\mathbf{g}_i\right|^2 + \sigma_u^2 \left\|\mathbf{f}_{u,k}\right\|_2^2}. \tag{34}$$

As we have indicated earlier, due to the large number of IIoT devices that transmit data simultaneously, reusing orthogonal RSs or using nonorthogonal RSs are necessary. In the following, we consider L group of IIoT devices and J UEs in each group.

We shall use double subscript (j,l) to identify a given IIoT device. So $\beta_{j,i}$ denotes the large scale fading between the base station service antenna array and the jth IIoT devices in the lth group. If we arrange all the users in a $J \times L$ matrix, each column of users then belongs to the same group, and therefore use mutually orthogonal RSs, and each row of users uses the same RSs. All the large-scale fadings is arranged in the following matrix.

$$\begin{aligned} B &= \begin{pmatrix} \beta_1 & \beta_2 & \cdots & \beta_L \\ \beta_{L+1} & \beta_{L+2} & \cdots & \beta_{2L} \\ \vdots & \vdots & \vdots & \vdots \\ \beta_{K-L+1} & \beta_{K-L+2} & \cdots & \beta_K \end{pmatrix} \\ &= \begin{pmatrix} \beta_{1,1} & \beta_{1,2} & \cdots & \beta_{1,L} \\ \beta_{2,1} & \beta_{2,2} & \cdots & \beta_{2,L} \\ \vdots & \vdots & \vdots & \vdots \\ \beta_{J,1} & \beta_{J,2} & \cdots & \beta_{J,L} \end{pmatrix}, \end{aligned} \tag{35}$$

This article has been accepted for publication in a future issue of this journal, but has not been fully edited. Content may change prior to final publication. Citation information: DOI 10.1109/TII.2017.2787988, IEEE Transactions on Industrial Informatics

With RS reuse, RS contamination is present. Assuming the mean-square channel estimate for the jth user in the lth group is $\gamma_{j,l}\beta_{j,l}$, $\gamma_{j,l}$ can be represented as:

$$\gamma_{j,l} = \frac{\tau_{\mathrm{p}}\rho_{\mathrm{u}}\beta_{j,l}}{1+\tau_{\mathrm{p}}\rho_{\mathrm{u}}\sum\limits_{l'=1}^{L}\beta_{j,l'}}, \tag{36}$$

Viewing the devices reusing RSs as devices in other cells, the multicell uplink SINR formulas derived in [12] can be applied to obtain the effective uplink SINR for single cell with RS reuse. Effective uplink SINR for single cell with RS contamination are written in expressions (37) and (38).

$$\mathrm{SINR}_{j,l}^{\mathrm{MR,ul}} = \frac{M\gamma_{j,l}\beta_{j,l}\rho_{\mathrm{u}}\eta_{j,l}}{\sum\limits_{j'=1}^{J}\sum\limits_{l'=1}^{L}\beta_{j',l'}\rho_{\mathrm{u}}\eta_{j',l'} + M\sum\limits_{\substack{l'=1\\l'\neq l}}^{L}\gamma_{j,l'}\beta_{j,l'}\rho_{\mathrm{u}}\eta_{j,l'} + \sigma_u^2}, \tag{37}$$

$$\mathrm{SINR}_{j,l}^{\mathrm{ZF,ul}} = \frac{(M-J)\gamma_{j,l}\beta_{j,l}\rho_{\mathrm{u}}\eta_{j,l}}{\sum\limits_{l'=1}^{L}\sum\limits_{j'=1}^{J}(1-\gamma_{j',l'})\beta_{j',l'}\rho_{\mathrm{u}}\eta_{j',l'} + (M-J)\sum\limits_{\substack{l'=1\\l'\neq l}}^{L}\gamma_{j,l'}\beta_{j,l'}\rho_{\mathrm{u}}\eta_{j,l'} + \sigma_u^2}. \tag{38}$$

In (37) and (38), $\eta_{j,l}$ is the power control coefficient for the jth user in the lth group. For the uplink, following condition must be met to satisfy individual power constraint.

$$\eta_{j,l} \leq 1, j = 1,\cdots,J,\ \ l = 1,\cdots,L, \tag{39}$$

To maintain moderate service to all the distributed IIoT devices, it is particularly important to design all the RX SNRs the same to reduce possible outage of some IIoT devices located far from the data center. For this, we use a simple power allocation strategy to ensure that all the IIoT devices have the same RX SNR.

$$\rho_{\mathrm{u}}\eta_{j,l} = \frac{\xi_{\mathrm{u}}}{\beta_{j,l}}, \tag{40}$$

where ξ is the signal power of each IIoT devices achieved at each BS antennas. The same power control can be performed for the downlink signal. Then, (37) and (38) can be simplified as follows:

$$\begin{aligned}\mathrm{SINR}_{j,l}^{\mathrm{MR,ul}} &= \mathrm{SINR}_{\mathrm{k,c}}^{\mathrm{MR,ul}} \\ &= \frac{M\xi_{\mathrm{u}}\gamma_{j,l}}{\xi_{\mathrm{u}}JL + M\xi_{\mathrm{u}}(L-1)\gamma_{j,l} + \sigma_u^2},\end{aligned} \tag{41}$$

$$\begin{aligned}\mathrm{SINR}_{j,l}^{\mathrm{ZF,ul}} &= \mathrm{SINR}_{\mathrm{k,c}}^{\mathrm{ZF,ul}} \\ &= \frac{(M-J)\xi_{\mathrm{u}}\gamma_{j,l}}{\xi_{\mathrm{u}}LJ(1-\gamma_{j,l}) + (M-J)\xi_{\mathrm{u}}(L-1)\gamma_{j,l} + \sigma_u^2}.\end{aligned} \tag{42}$$

The downlink SINR can also be derived in the similar manner. From the previous section, the downlink precoder can be shown as follows.

$$F_{\mathrm{d}} = \begin{cases} \hat{H}^* D_{\hat{H}^{\dagger}\hat{H}}^{-1/2} D_{\eta}^{1/2} & \text{for MRC} \\ \sqrt{\hat{c}_1}\hat{H}^*(\hat{H}^{\mathrm{T}}\hat{H}^*)^{-1} D_{\eta}^{1/2} & \text{for ZF} \\ \sqrt{\hat{c}_2}\hat{H}^*\left(\hat{H}^{\mathrm{T}}\hat{H}^* + \Gamma_d^{-1} I_K\right)^{-1} D_{\eta}^{1/2} & \text{for MMSE} \end{cases} \tag{43}$$

where $\hat{c}_1$ and $\hat{c}_2$ are normalization factors for ZF and MMSE precodings based on the estimated channel. For ZF, J must satisfy $J < M$.

The downlink RX signal from data center to the distributed IIoT devices can be represented as

$$\begin{aligned} y &= \sum_{i=1}^{K}\sqrt{\rho_{\mathrm{d,i}}}\mathbf{h}_i^{\mathrm{T}}\cdot\mathbf{f}_{d,k}x_i + \mathbf{w} \\ &= \underbrace{\sqrt{\rho_{\mathrm{d,k}}}\mathbf{h}_k^{\mathrm{T}}\cdot\mathbf{f}_{d,k}x_k}_{\text{Desired signal}} + \underbrace{\sum_{\substack{i=1\\i\neq k}}^{K}\sqrt{\rho_{\mathrm{d,i}}}\mathbf{h}_i^{\mathrm{T}}\cdot\mathbf{f}_{d,k}x_i}_{\text{Inter-User Interference}} + \underbrace{\mathbf{w}}_{\text{Noise}}, \end{aligned} \tag{44}$$

where $\rho_{\mathrm{d,i}} = \rho_{\mathrm{d}}\eta_i$ is the TX power to ith UE. Based on (44), we can derive the downlink SINR for kth UE [11] [12] [13].

$$\mathrm{SINR}_{\mathrm{k}}^{\mathrm{dl}} = \frac{\rho_{\mathrm{d,k}}\left|\mathbf{h}_k^{\mathrm{T}}\mathbf{f}_{d,k}\right|^2}{\sum\limits_{\substack{i=1\\i\neq k}}^{K}\rho_{\mathrm{d,i}}\left|\mathbf{h}_i^{\mathrm{T}}\mathbf{f}_{d,k}\right|^2 + \sigma_d^2}. \tag{45}$$

The closed form of downlink SINR can be represented as similar manner with the uplink SINR.

The effective SINRs for very comprehensive Massive MIMO systems are given in [11] and [12]. The effective SINR for Massive MIMO in LoS propagation is given in [13]. These SINR expressions greatly facilitates the performance analysis of Massive MIMO, and can be adapted to treat the applications of Massive MIMO in IIoT.

Let us observe how the RS reuse based Massive MIMO with massive connectivity is working for IIoT network. The performance can be observed using the derived SINRs. The uplink and downlink SE can be represented as

$$\mathrm{R}^{\mathrm{u}} = \sum_{i=1}^{\chi^{\mathrm{u}}}\zeta^{\mathrm{u}}\left(1-\frac{\tau_p}{\tau_c}\right)\log_2(1+\mathrm{SINR}_{\mathrm{i}}^{\mathrm{ul}}). \tag{46}$$

$$\mathrm{R}^{\mathrm{d}} = \sum_{i=1}^{\chi^{\mathrm{d}}}\zeta^{\mathrm{d}}\left(1-\frac{\tau_p}{\tau_c}\right)\log_2(1+\mathrm{SINR}_{\mathrm{i}}^{\mathrm{dl}}). \tag{47}$$

where χ^{u} and χ^{d} are the adjustable factors to reflect the number of coincidently supported UEs for uplink and downlink transmission each, ζ^{u} and ζ^{d} are the parameters to reflect the actual data transmission resource slot for uplink and downnlink, i.e., $\zeta^{\mathrm{u}} + \zeta^{\mathrm{d}} = 1$. In this paper, we assume that a half of τ_c is dedicated to the uplink RS at the maximum, and the rest half of τ_c is dedicated to the data transmission. Also, a half of data transmission portion is dedicated to the uplink data transmission, i.e., $\zeta^{\mathrm{u}} = \zeta^{\mathrm{d}} = 0.5$.

The simulation parameters used in this paper are presented in Table II.

This article has been accepted for publication in a future issue of this journal, but has not been fully edited. Content may change prior to final publication. Citation information: DOI 10.1109/TII.2017.2787988, IEEE Transactions on Industrial Informatics

TABLE II
SIMULATION PARAMETERS

Parameter	Value
Coherence Time, τ_c	10, 50 msec
Coherence Bandwidth, BW_c	210kHz
RS time, τ_p	5, 25msec
Total symbols in coherence interval, S_{tot}	1960, 9800
Max. number of groups, L_{max}	5, 2
Max. number of UEs in each group, J_{max}	980, 4900
Max. total number of UEs, K_{max}	9800
Portion of data trans. resource slot, ζ^u,ζ^d	0.5
Max. number of serviced UEs for uplink, χ^u_{max}	9800
Max. number of serviced UEs for downlink, χ^d_{max}	100, 9800
UL SNR per UE	0, 5 dB
DL SNR	10 dB

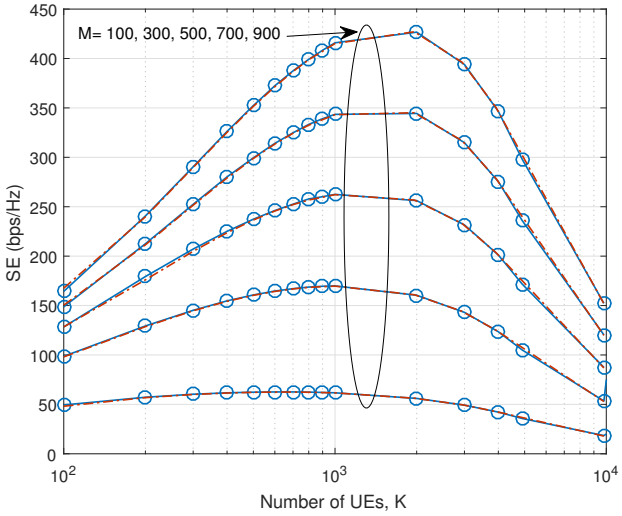

Fig. 3. Uplink SE (bps/Hz) using MR processing versus number of UEs, K, SNR = 0 dB, $\tau_c = 50$msec.

Fig. 3 shows the uplink SE using MR precessing. The dotted line indicates the closed form results of SINR which are well-matched to the simulation results. We assume 50 msec coherence time which can be applicable to the nomadic and static UEs, and 210kHz coherence bandwidth, BW_c. Assuming BW of one resource element is 15kHz, there are $196 \times 50 = 9800$ total symbols, S_{tot} in a coherence interval. We use the $9800/2 = 4900$ symbols for the uplink RS at the maximum, that is $J_{max} = 4900$. If K is smaller than 4900, the uplink RS can be smaller than 4900 symbols, then the resources for the data transmission can be increased. We make the SNR from each IIoT devices 0 dB at RX. Since the maximum number of UEs, K_{max} is 9800, L_{max} is $\lceil \frac{K_{max}}{J_{max}} \rceil = 2$. As observed, if K increases, SE gradually increases, and decreases after a certain point and/or RS reuse. SINR becomes worse as K and/or L increases. However, for MR processing, χ^u increases as K and/or L increases. Therefore, the Massive MIMO equipped data center can support much greater numbers of IIoT devices with little SE loss and outage. Increasing M in data center is always beneficial.

We present the SINR distribution of uplink MR processing in Fig. 4. As K increases, interference also increases, thus SINR becomes worse. The RS reuse is started from $K = 4900$.

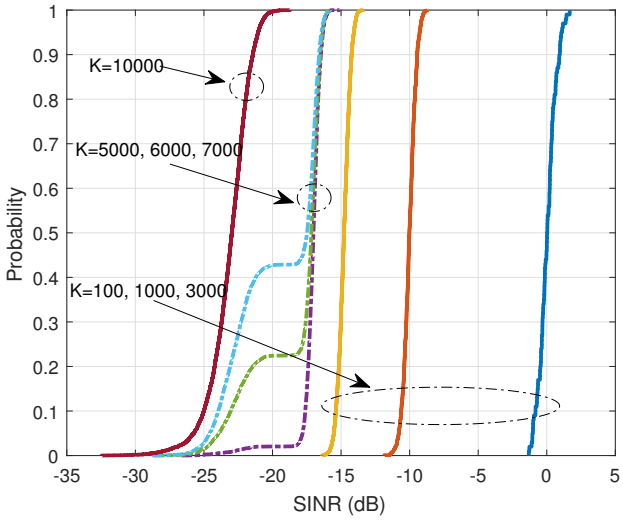

Fig. 4. CDF of SINR (dB): Uplink with MR processing. $M = 100$ and $\tau_c = 50$msec.

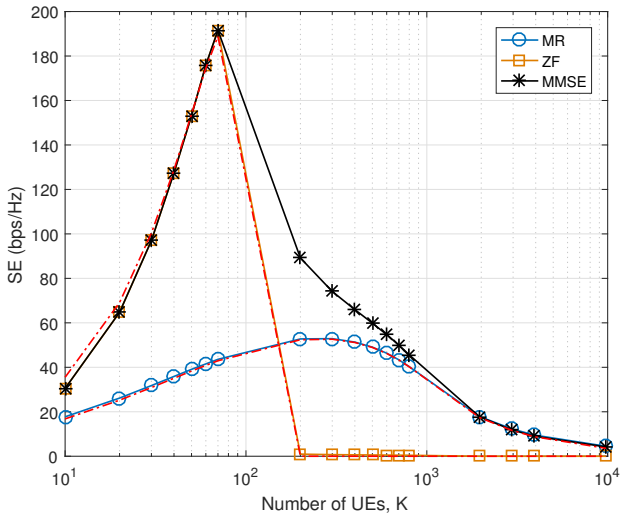

Fig. 5. Uplink SE (bps/Hz) versus number of UEs, K, when SNR = 5 dB, $M = 100$, and $\tau_c = 10$msec.

The abrupt SINR changes of $K = 5000$, 6000, and 7000 are due to the RS reuse interference of some UEs in a given group.

ZF processing are very sensitive to the channel estimation error, and thus it is not well-fitted to the massive connectivity with a large number of K. Fig. 5 shows the uplink SE (bps/Hz) versus number of UEs, K, when uplink SNR = 5 dB. In this simulation, we choose $\tau_c = 10$msec to show the effectiveness of RS reuse ($L_{max} = 5$). As K and/or L increases, the SE of ZF processing reaches outage. This is due to the fact that RS reuse increases the channel estimation error, and in the case of ZF, there is not enough degrees of freedom to perform zero-forcing when $K > M$. Increasing TX power and/or SNR for each device cannot recover it from outage. On the other hand, for the MR processing, as L increases, SE gradually decreases. This phenomenon is maintained in the case of very low SNR. MMSE processing also presents a good performance. When there are a lot of UEs ($K > 1000$), it shows similar performance to MR processing. However, the complexity and delay of

This article has been accepted for publication in a future issue of this journal, but has not been fully edited. Content may change prior to final publication. Citation information: DOI 10.1109/TII.2017.2787988, IEEE Transactions on Industrial Informatics

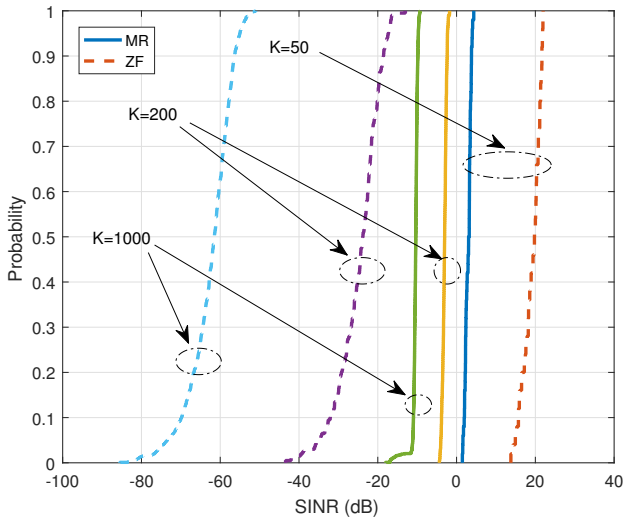

Fig. 6. CDF of Uplink SINR (dB): $M = 100$ and $\tau_c = 10$msec.

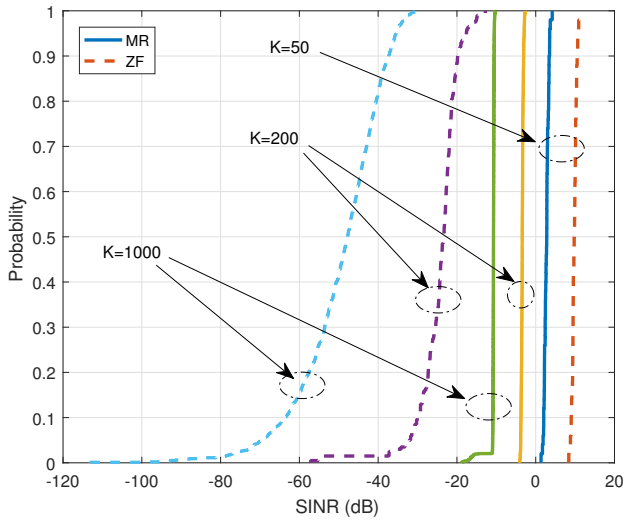

Fig. 8. CDF of Downlink SINR (dB): $M = 100$ and $\tau_c = 10msec$.

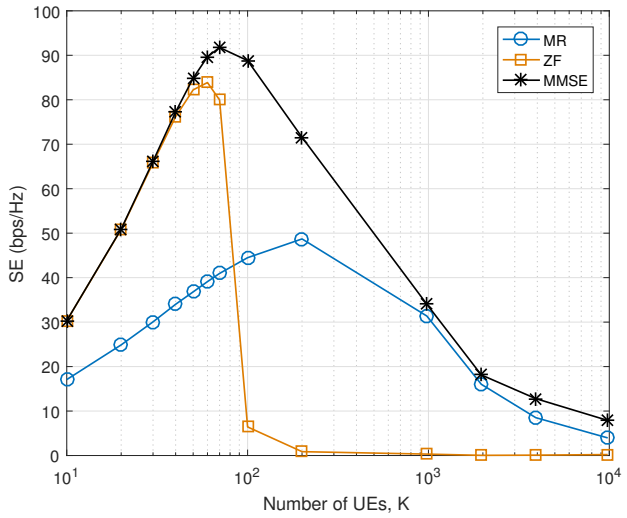

Fig. 7. Downlink SE (bps/Hz) versus number of UEs, K, when uplink SNR = 5 dB, downlink SNR = 10dB, $M = 100$, and $\tau_c = 10$msec.

MMSE processing should be carefully considered. Therefore, for the uplink of Massive MIMO with massive connectivity, MR processing can be a good choice.

Fig. 6 shows the SINR comparison between MR processing and ZF processing. The SINR of ZF preocessing is better than MR processing, when $M > K$. However, when $M < K$, SINR of MR processing becomes much better than ZF processing. In particular, When $K = 1000$, the SINR difference between MR processing and ZF processing is more than 50dB which is another proof that ZF processing does not give any meaningful performance to support massive IIoT devices.

Now, let us look at the case of the downlink in Fig. 7. Downlink SE heavily depends on the accuracy of uplink channel estimation because the downlink precoder is generated based on the estimated uplink channel. Increasing uplink SNR improves the channel estimation accuracy, and thus improve the downlink SE. However, RS reuse decreases the accuracy of channel estimation. Increasing K decreases the downlink SE. When there are a lot of UEs ($K > 1000$), MMSE precoding shows similar performance to MR precoding, but again, the complexity and delay of MMSE precoding should be carefully considered. Therefore, using MR processing/precoding, the RS reuse Massive MIMO with massive connectivity scheme can be well applicable to low cost IIoT network systems with little delay.

The SINR comparison between MR precoding and ZF precoding for downlink signal is shown in Fig. 8. As observed, SINR of MR precoding is much better than ZF precoding, when $K > M$. Uplink SNR depends on the TX power of each UE, while downlink SNR depends on the total TX power of BS, which is shared among all the UEs. Similar to the uplink case, when $K = 1000$, the SINR difference between MR precoding and ZF precoding is more than 50dB.

The analysis in this section shows the single cell case with one base station and many IIoT devices. However, in the IIoT network, it could be more effective to have many base stations and multiple cells with reliable scheduling depending on applications. In this case, the IIoT network can be very similar to the cellular network. The schemes in the cellular network can be used for the IIoT network when high reliability and data rate are necessary. However, in this case, a great deal of cost is required, thus it could be unsuitable for some of the IIoT network which requires low cost. The system we are introducing in this paper only uses one base station with no scheduling. The system is not a performance centric system, but a cost centric one. As observed, the proposed scheme can maintain moderate data rate even though the simultaneous support of quite a large number of IIoT devices. Therefore, the proposed scheme can be successfully applied to the IIoT networks which requires moderate data rate with low cost.

What we showed here is the feasibility of Massive MIMO with massive IIoT device connectivity. The term, “industrial” can be better fitted to the high reliablity system depending on the situation. Thus, in general, our system can be also well-fitted to the general IoT network. There are many situations to support the IIoT network. We shall discuss the research challenges and applications of Massive MIMO in a variety of

This article has been accepted for publication in a future issue of this journal, but has not been fully edited. Content may change prior to final publication. Citation information: DOI 10.1109/TII.2017.2787988, IEEE Transactions on Industrial Informatics

IIoT networks in the next section.

Since Massive MIMO has an excessive amount of service antenna, it can efficiently gather big data with its many service antennas. The specific application could be gathering data from a smart factory surveillance system that monitors the operation of entire smart factory system, and from an underwater/coastal surveillance system that monitors the changes of ecosystems. The specific system setup can be discussed in future works.

IV. Research Challenges and Discussions on Industrial Applications of Cyber-Physical System using Massive MIMO

In this section, we present possible research topics of Massive MIMO for the application of industrial internet in CPS, and provide related discussions. We categorize the possible research challenges as scheduling and power control, channel estimation and calibration, RS reuse in multi-cell scenario, energy efficiency design and energy transfer/harvesting, signaling techniques for drones and mobile robots, and application for an underwater industrial internet. Scheduling and power control are related to basic operations of Massive MIMO to transmit the data efficiently. For the industrial internet, the operation cost is one of the most important factors. For this reason, energy efficient design and RF energy transfer/harvesting can be two must-have core technologies. Since Massive MIMO employs closed-loop beamforming, a relatively short coherence interval must be used for fast moving users. There are several fast moving targets in the industrial internet domain. The methods for concurrently supporting stationary and moving targets, such as drones and mobile robots are very important research topics for the success of Massive MIMO based CPS. The importance of underwater IIoT is growing, but little work has been done. Developing underwater IIoT is a challenging work. If we use Massive MIMO, the limited bandwidth in underwater can be compensated using parallel spatial transmission, and thus Massive MIMO can also be a good solution for an underwater industrial internet.

A. Scheduling and Power Control

Typically, MIMO scheduling is performed when there are more UEs than the number of BS service antennas. The selection of UEs that receive the data signal at each interval is based on the channel characteristic of each UE. The data center finds the best combination of UEs based on the channel characteristics to increase throughput and/or efficiency. Generally, to find the optimum case, it requires heavy computations which may cause delays.

In the traditional Massive MIMO assumption, the number of service antennas in data center is much greater than the number of antennas in UEs (e.g., $M > 10K$), and so scheduling for UE selection is not necessary. Due to the channel hardening effect, fast power control in the scale of fast fading is of little help to improve the efficiency. Comparing to the the case of the cellular system, where the environment is assumed to be fully random in the sense that user locations and their mobilities are randomly distributed, in the case of the industrial internet system, it may be possible to adjust the environment somewhat, and limit the UEs' locations and moving ranges under operation. The UEs may be classified as moving targets and fixed targets depending on the situation. The scheduling and power control of Massive MIMO for industrial internet application can be based on the importance of UEs data. Unlike the cellular environment which does not have highly premium users, for the hyper-connectivity of industrial internet, some critical data can be much more important than others. In this situation, we can reduce the number of target UEs, and increase the reliability of the data based on the channel gain coming from the difference between M and K. In the case of $K > M$, we have already witnessed that the RS reuse system can be well established with MR processing.

Recently, an interesting scheme to control many IoT devices has been introduced [14]. In that scheme, the authors used a hybrid periodic-random massive access (HPRMA) scheme for wireless clinical networks employing ultra-narrow band (UNB) techniques. In particular, the proposed scheme targets accommodating a large population of devices with several new features. It can dynamically adjust the resource allocated for coexisting periodic and random services based on the traffic load learned from signal collision status. It can be also considered that these schemes can be combined with Massive MIMO to support many IIoT devices.

B. Channel Estimation and Calibration

The channel estimation for Massive MIMO is a traditional problem, and much related research can be found in the literature. The importance of channel estimation in the proposed scheme is more important than traditional Massive MIMO because the system we propose employs RS reuse. Several channel estimation methods for RS reduction and/or reuse have been reported. Blind channel estimation technologies using the specific statistical property of the signal and the channel, and the correlation based channel recovery were introduced in [15] [16]. This kind of technology can have very high impact, but it usually requires long observation time and high complexity. Training based super imposed RS on data signal, which locates the RS stream and data stream in same resources, were also introduced in [17] [18]. This can give very efficient results for reducing RS overhead, because data can be transmitted in all time and frequency resources. However, the performance loss due to data and RS imposition is inevitable. Channel estimation in RS reuse situation is very challenging and important topic to deal with.

Also, channel estimation in Massive MIMO necessarily requires channel calibration. As mentioned, due to a large number of service antennas, Massive MIMO should use TDD mode. To estimate downlink channel from uplink channel, highly reliable channel calibration is an essential technique to achieve [19] [20] [21] [22].

C. RS reuse in Multi-cell Scenario

IIoT devices are continually growing, and it is highly possible that single cell RS reuse and/or multi-cell orthogonal RS may not be enough depending on situations. The unprecedented growth in IoT communications is predicted to

This article has been accepted for publication in a future issue of this journal, but has not been fully edited. Content may change prior to final publication. Citation information: DOI 10.1109/TII.2017.2787988, IEEE Transactions on Industrial Informatics

accumulate to over 20 billion connected IoT devices by the year 2020 [23]. Possibly facing such a reality, it is highly possible that a multi-cell Massive MIMO system with heavy RS reuse or using nonorthogonal RS will be necessary. In this case, there can be three kinds of interference: intra-cell interference; multi-cell interference; RS reuse/nonorthogonal RS interference. The system would be quite complicated, but it can support an enormous number of IIoT devices with moderate data rate. Designing and investigating this kind of system will be a quite challenging research topic.

D. Energy Efficiency Design, RF Energy Transfer and Harvesting

Energy efficient industrial internet design and cognitive wireless based energy harvesting research can be promising items.

1) Energy Efficiency Design: It is well-known that most communication systems use spectral efficiency (SE) or throughput (TP) as a performance metric. However, EE could be more important than SE depending on the applications. In particular, increasing EE in industry is directly connected to the operation price.

Although SE has been used as a performance metric for a long time, the current form is insufficient for certain applications. The reason is that SE does not reflect power consumption related performance. For example, from SE perspective, increasing TX power is always beneficial, but that is not true in real systems when operating cost is taken into account. For this reason, the EE performance metric can be defined as the ratio of TP to power consumption:

$$EE \triangleq \frac{B\sum_k R_k}{P_{\text{total}}}. \tag{48}$$

where P_{total} is the total of power consumption, B is the system bandwidth, R_k is the SE for UE k. Basically, EE is defined as sytem total TP divided by total power consumption. P_{total} can include only important system power consumption factors. The continuous increase of power consumption can increase SE only up to a certain point which is in the power limited region. Beyond the power limited region there will be only marginal increase in SE, and in some situation there may even be negative effect due to self interference. Finding an optimal operating point to balance the EE and SE benefits is often a very challenging and interesting research task.

2) RF Energy Transfer and Harvesting: RF energy transfer and harvesting techniques have recently become amazing technologies for distributed wireless sensor networks [24]. Industrial internet is also a kind of distributed sensor networks, thus transferring energy using RF signal to the remotely distributed UEs can give significant benefit for the operation of industrial internet. Due to the serious battery limitation of sensors, studies on the energy harvesting method based on the RF power transmission using Massive MIMO is a very promising research field. Interference signal can be used as a source of energy harvesting when the interference is high. This kind of logic can be applicable to cognitive radio systems. Secondary user can use the primary user's signal as a RF energy harvesting source.

Wireless power transmission basically requires a receiving RF power of at least -20dBm [24], so it is necessary to design a mechanism to perform RF energy transmission by bringing a monitoring drone or a mobile robot close to sensors. RF energy transfer is performed using 300GHz to 3kHz frequency range of electromagnetic radiation. Since the RF power strength is attenuated according to the cube of the reciprocal of distance, only close UEs can be directly supported. Some of antennas can be selected as RF energy sources based on antenna selection schemes. For the UEs whose energy consumption cannot directly be supported by Massive MIMO, surveillance drones can be a good medium to transfer RF energy. The drone can closely approach to the Massive MIMO data center, and receive RF energy from the data center, then move close to the UEs that requires RF energy, and transfer the RF energy to the UEs. This kind of mechanism can be well-designed for the high sustainability industrial internet networks. The energy efficiency of the IIoT network is very important because it is closely related to operational cost. The feasibility of using drones as energy medium can be analyzed based on power consumption modeling of Massive MIMO equipped IIoT network systems with drones. In case of emergencies, the RF energy beamforming technique can be used for the UEs using the large number of antennas in Massive MIMO [25]. Simultaneous wireless information and power transfer (SWIPT) has also been proposed for delivering RF energy and wireless information concurrently, which offers a low-cost option for sustainable operations of wireless systems without hardware modification on the transmitter side [24] [26].

E. Signaling Techniques for Drones and Mobile Robots

There are some moving targets, such as drones and mobile robots, for the industrial internet, and the importance of supporting these targets is increasing. The drone should be connected to a data center to transmit/receive surveillance data. To control drones using Massive MIMO, there are various issues to consider. Since drones are aerially located, most of the channels are line-of-sight (LoS). If several drones are located together, then there could be a problem due to beam collision/high correlation. However if drones are separated, thanks to the angle difference, multiple drones can be supported without any problem. According to the recent study, in the case of $M = 100$ and $K = 12$, the sum capacity in the LoS case is similar to that of rich scattering in the majority of cases, but there is a 10 percent risk that the LoS performance loss is more than 10 percent [7]. One of the important topics in drone control is auto-landing. Ultra-wide band (UWB) based auto-landing research has been actively studied. Using Massive MIMO, UWB signal can be transmitted from some of antennas to support the auto-landing of the drone nearby data center [27].

Generally, Massive MIMO is well suited for nomadic/static UEs. There may not be so many fast moving targets for industrial internet application. However, if those kinds of targets exist, then based on the expected moving track of the target, it may be possible to make a tracking beam to support fast moving targets, especially for devices with well-defined trajectories.

This article has been accepted for publication in a future issue of this journal, but has not been fully edited. Content may change prior to final publication. Citation information: DOI 10.1109/TII.2017.2787988, IEEE Transactions on Industrial Informatics

F. Underwater industrial internet

In recent years, research on the underwater industrial internet has been actively pursued for the purposes of monitoring climate change and water environment, offshore oil/gas exploration, military defense systems, remote operations utilizing autonomous underwater vehicle/robot for the resource exploration, and life-saving, etc. Unlike the terrestrial communication systems, underwater communication systems suffers a very high path loss when using electromagnetic waves. To cope with this problem, acoustic waves are typically used for underwater communication systems for relatively long distance communications. Also, blue optical light can be used because it is attenuated the least of all electromagnetic radiations.

We can say there are three distinct underwater channel characteristics. First, absorption loss drastically increases as frequency band increases. We recognize this characteristic as bandwidth limitation. This can causes serious inter-symbol interference. Second, underwater channel shows the serious doubly selectivity, i.e., both time and frequency selectivity. There are serious multipaths due to underwater mediums, and this condition is continuously changing due to the floatation and movement of the medium. Third, if we use acoustic waves, the speed is very slow, typically 1,500m/s, and it is 200,000 times slower than terrestrial communication systems which typically use electromagnetic waves. Due to the these distinct characteristics of underwater channel, there are many challenges in maintaining hyper-connectivity for the underwater CPS.

Massive MIMO can also play a distinct role for the hyper connectivity of underwater CPS. One of advantages in the underwater industrial internet system is that there is less space limitation compared to terrestrial systems. Typically, we can secure plenty of room for underwater Massive MIMO antenna systems. Since underwater systems have serious bandwidth limited constraint, securing more space is very useful because it can compensate the limited band using parallel space transmission. Moreover, if we use visible light communications (VLC) for CPS, the size of the Massive MIMO antenna array becomes very small, and it can be an additional advantage for some underwater systems. Typical modulation choice could be orthogonal frequency division multiplexing (OFDM). For long distance connectivity, acoustic waves can be used. Even though there is a plenty of room in underwater, it could be difficult to deploy acoustic wave based Massive MIMO due to high price and huge size. For the industrial internet, the range of connectivity is smaller than several hundred meters. Thus, light and/or electromagnetic waves can be adopted. In this case, the number of antennas can be several hundred or more. There was one study indicating transmission the RF wave at 100kbps over tens of meters [28]. It requires huge and high capability receiver devices, thus more study is necessary to be used for underwater industrial internet. The switchable beamforming technique could also be appropriately applied to support multi-target hyper connectivity. Random beamforming could be very helpful to support many underwater IIoT devices.

V. Conclusions

In this paper, we introduced the Massive MIMO for the CPS based industrial internet. The number of devices for the industrial internet is growing rapidly, and there needs to be a high capacity communication system that can reliably support many IIoT devices. In this regard, Massive MIMO can support many IIoT devices with high reliability. In this paper, we have presented two contributions: First, we have addressed several key issues of applying Massive MIMO to IIoT, for example, we have carried out detailed investigations on the performance of three well-known linear processing techniques when a large number of devices are to be served simultaneously. The related SINR analysis can greatly help to better understand this newly introduced system. Second, we have provided an overview of research topics and challenges of the IIoT network system with Massive MIMO. The related discussions can serve as a good starting point for the research of this important field in the true IoT era. CPSs are truly large computer-controlled systems, and there are three core technologies that constitute CPS, i.e., communication, computation, and control. To support hyper connectivity through the communication technology, Massive MIMO can be a core technology because of its high SE and EE. The initial concept of Massive MIMO has been actively studied in the cellular environment, but its distinct characteristic can also be well suited for industrial internet applications. Supporting various IIoT devices through many service antennas in a data center is a typical form of Massive MIMO system. Scheduling and power control are much simpler thanks to the channel hardening effect. On the other hand, to support massive connectivity of IIoT devices, RS reuse should be applicable depending on the specific situation at hand. Thus, possibility of RS reused system has been shown, and as observed, Massive MIMO can support many IIoT devices based on RS reuse. In addition to that, there are many research topics for the industrial internet using Massive MIMO. Since operation cost is one of the most important factors for industrial internet, design of energy efficient industrial Massive MIMO is very important. Also RF energy transfer and harvesting can be of great help for the battery limited IIoT devices. For moving targets, including drones and mobile robots, it was already discussed that LoS does not so much degrade the data rate due to the separated and limited number of UEs. Industrial Massive MIMO also fits well with the underwater application because it can compensate the bandwidth limitation using the parallel transmission. Underwater VLC using Massive MIMO beamforming is a good IIoT application. In this case, the size of the antenna array is not a problem. The discussions in this paper can serve as a good starting point for the industrial internet application of Massive MIMO.

References

[1] W. Wolf, "Cyber-physical systems," *Computer* 42 (3), pp.88-89, 2009.
[2] E.A. Lee, "Cyber physical systems: Design challenges," *2008 11th IEEE International Symposium Object Oriented Real-Time Distributed Computing (ISORC),* pp.363-369, 2008.
[3] R. R. Rajkumar, I. Lee, L. Sha, J. Stankovic, "Cyber-physical systems: the next computing revolution," *In Proceedings of the ACM 47th Design Automation Conference,* pp. 731-736, June 2010.

[4] L. D. Xu, W. He, S. Li, "Internet of Things in Industries: A Survey," *IEEE Trans. Ind. Informat.*, , vol. 10, no. 4, pp.2233-2243, Nov. 2014.
[5] F. G. Brundu, E. Patti, A. Osello, M. Del Giudice, N. Rapetti, ' A. Krylovskiy, M. Jahn, V. Verda, E. Guelpa, L. Rietto, A. Acquaviva, "IoT Software Infrastructure for Energy Management and Simulation in Smart Cities," *IEEE Trans. Ind. Informat.,* vol. 13, no. 2, pp.832-840, April 2017.
[6] T. L. Marzetta, "Noncooperative Cellular Wireless with Unlimited Numbers of Base Station Antennas," *IEEE Trans. Wireless Commun.*, vol. 9, no. 11, pp. 3590-3600, Nov. 2010.
[7] E. Bjornson, E. G. Larsson, T. L. Marzetta, "Massive MIMO: ten myths and one critical question," *IEEE Commun. Mag.*, vol.54, no. 2, pp. 114-123, Feb. 2016.
[8] T. L. Marzetta, "Massive MIMO: An Introduction," *Bell Labs Technical Journal*, vol. 20, pp. 11-22, 2015.
[9] H. Ji, Y. Kim, J. Lee, E. Onggosanusi, Y. Nam, J. Zhang, B. Lee, and B. Shim, "Overview of Full-Dimension MIMO in LTE-Advanced Pro," *IEEE Commun. Mag.,* vol. 55, pp. 176-184, Feb. 2017.
[10] B. M. Hochwald, T. L. Marzetta, and V. Tarokh, "Multiple-antenna channel hardening and its implications for rate feedback and scheduling," *IEEE Trans. on Information Theory*, vol. 50, no. 9, pp. 1893-1909, 2004.
[11] T. V. Chien and E. Bjrnson, "Massive MIMO Communications," in 5G Mobile Communications, W. Xiang et al. (eds.), pp. 77-116, Springer, 2017.
[12] T. L. Marzetta, E. G. Larsson, H. Yang, and H. Q. Ngo, *Fundamentals of Massive MIMO*, Cambridge Univ. Press, London 2016.
[13] H. Yang and T. L. Marzetta, "Massive MIMO with max-min power control in line-of-sight propagation environment," *IEEE Trans. Commun.*, vol. 65, no. 11, pp. 4685-4693, Nov. 2017.
[14] Q. Du, W. Zhao, W. Li, X. Zhang, B. Sun, H. Song, P. Ren L. Sun, and Y. Wang, "Massive Access Control Aided by Knowledge-Extraction for Co-Existing Periodic and Random Services over Wireless Clinical Networks," *Journal of Medical Systems,* 40:171, July 2016.
[15] A.P. Petropulu; R. Zhang; R. Lin, Blind OFDM Channel Estimation through Simple Linear Precoding, *IEEE Trans. on Wireless Commun,* vol. 3, no. 2, pp. 647-655, March 2004.
[16] C. Shin; R. W. Heath; E. J. Powers, Blind channel estimation for MIMO-OFDM systems, *IEEE Trans. on Vehicular Tech.,* vol. 56, issue 2 pp.670-685, March 2007.
[17] M. Coldrey; P. Bohlin, Training-Based MIMO SystemsPart I: Performance Comparison, *IEEE Trans. on Signal Proc.,* vol. 55, issue 11, pp.5464-5476, Nov. 2007.
[18] M. Coldrey; P. Bohlin, Training-Based MIMO Systems: Part II Improvements Using Detected Symbol Information, *IEEE Trans. on Signal Proc.,* vol. 56, issue 1, pp.296-303, Jan. 2008.
[19] B. M. Lee, "Calibration for Channel Reciprocity in Industrial Massive MIMO Antenna Systems," *IEEE Trans. Ind. Informat.,* DOI: 10.1109/TII.2017.2749431, Sept. 2017.
[20] H. Wei, D. Wang, H. Zhu, J. Wang, S. Sun, and X. You, "Mutual Coupling Calibration for Multiuser Massive MIMO Systems," *IEEE Trans. Wireless Commun.,* vol. 15, no. 1, pp. 606-619, Jan. 2016.
[21] C. Shepard, H. Yu, N. Anand, L.E Li, T.L. Marzetta, R. Yang, and L. Zhong, "Argos: Practical many-antenna base stations," *in Proceedings of the 18th Annual International Conference on Mobile Computing and Networking, Mobicom 12.*, New York, NY, USA, pp. 53-64, 2012.
[22] F. Kaltenberger, H. Jiang, M. Guillaud, and R. Knopp, "Relative channel reciprocity calibration in MIMO/TDD systems," *in Future Network and Mobile Summit,* pp.1-10, June 2010.
[23] S. Mumtaz, A. Alsohaily, Z. Pang, A. Rayes, K. F. Tsang, and Jonathan Rodriguez, "Massive Internet of Things for Industrial Applications: Addressing Wireless IIoT Connectivity Challenges and Ecosystem Fragmentation," *IEEE Ind. Electron. Mag,* vol. 11, issue 1, pp.28-33, Mar. 2017.
[24] X. Lu, P. Wang, D. Niyato, D.I. Kim, Z. Han, "Wireless Networks With RF Energy Harvesting: A Contemporary Survey," *IEEE Commun. Surveys Tuts.,* vol.17, no.2, Second Quarter, 2015.
[25] X. Chen, X. Wang, and X. Chen, "Energy-efficient optimization for wireless information and power transfer in large-scale MIMO systems employing energy beamforming," *IEEE Wireless Commun. Lett.,* vol. 2, no. 6, pp. 667-670, Dec. 2013.
[26] R. Zhang and C. K. Ho, "MIMO broadcasting for simultaneous wireless information and power transfer," *IEEE Trans. Wireless Commun.,* vol. 12, no. 5, pp. 1989-2001, May 2013.
[27] E. Kim, D. Choi, "A UWB positioning network enabling unmanned aircraft systems auto land," *Aerospace Science and Technology,* 58, pp.418-426, Nov. 2016.
[28] H. Brundage, "Designing a Wireless Underwater Optical Communication System," Master of Science in Mechanical Engineering, Massachusetts Institute of Technology, 2010.

Byung Moo Lee (M'05) received the Ph.D. degree in Electrical and Computer Engineering from the University of California, Irvine, CA, USA, in 2006. He is currently an Assistant Professor in the School of Intelligent Mechatronics Engineering at Sejong University, Seoul, Korea. Prior to joining Sejong University, he had 10 years of industry experience including research positions at the Samsung Electronics Seoul R&D Center, Samsung Advanced Institute of Technology (SAIT), and Korea Telecom (KT) R&D Center. During his industry experience, he participated in IEEE 802.16/11, Wi-Fi Alliance, and 3GPP LTE standardizations, and also participated in Mobile VCE and Green Touch Research Consortiums where he made numerous contributions and filed a number of related patents. His research interests are in the areas of wireless communications, signal processing, and machine learning applications. Dr. Lee served as a Vice Chairman of the Wi-Fi Alliance Display MTG in 2015-2016.

Hong Yang received the Ph.D. degree in Applied Mathematics from Princeton University, Princeton, NJ, USA. He worked in academia and for a start-up network technology company before joining Lucent Technologies and Alcatel-Lucent, where he was with the Wireless Design Center, the Systems Engineering Department, and the Bell Labs Research. He is currently a Member of Technical Staff with the Mathematics of Networks and Communications Research Department, Nokia Bell Labs, Murray Hill, NJ, USA, where he conducts research in communications networks. He has co-authored many research papers in wireless communications, applied mathematics, control theory, and financial economics. He co-invented many U.S. and international patents. He co-authored the book Fundamentals of Massive MIMO (Cambridge University Press, 2016).